

# Electron reconstruction in simulated Pb+Pb events in CMS

by

Yi Chen

Submitted to the Department of Physics  
in partial fulfillment of the requirements for the degree of

Bachelor of Science in Physics

at the

MASSACHUSETTS INSTITUTE OF TECHNOLOGY

June 2008

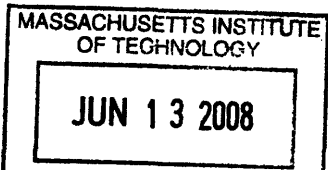
© Yi Chen, MMVIII. All rights reserved.

The author hereby grants to MIT permission to reproduce and  
distribute publicly paper and electronic copies of this thesis document  
in whole or in part.

Author .....  
/ Department of Physics  
May 16, 2008

Certified by.....  
Gunther Roland  
Associate Professor in the Department of Physics  
Thesis Supervisor

Accepted by .....  
David E. Pritchard  
Professor, Senior Thesis Coordinator, Department of Physics





## Acknowledgments

First of all I would like to thank professor Gunther Roland for supervising my thesis and, most of all, the guidance and training during the two years in which I stayed in this group. I would also like to thank Yen-jie Lee, who gave me a lot of advice on the possible ways to progress on the study. Finally I would like to thank my advisor, professor Wit Busza, and everyone who helps me with my studies at MIT and made the undergraduate studies here a pleasant experience.



## Contents

|  |           |
|--|-----------|
| <b>1. Introduction</b>   | <b>7</b>  |
| <b>2. Production rates at LHC</b>  | <b>9</b>  |
| <b>3. Simulated Samples</b>  | <b>10</b> |
| 3.1. Simulation, Mixing and Digitization                                 | 13        |
| <b>4. Reconstruction Procedure</b>                                       | <b>14</b> |
| 4.1. Supercluster Reconstruction   | 14        |
| 4.2. Tracker Reconstruction for Electrons                                | 15        |
| 4.3. Cuts Used to Select Electrons                                       | 16        |
| 4.4. Background Subtraction  | 21        |
| 4.5. Back-extrapolation  | 21        |
| <b>5. Simple Reconstruction Properties</b>                               | <b>22</b> |
| 5.1. Electromagnetic Calorimeter   | 22        |
| 5.2. Electron  | 23        |
| 5.3. Electron tracking in Heavy ion Background                           | 24        |
| <b>6. Background Particles</b>   | <b>25</b> |
| <b>7. Reconstructing <math>Z^0</math> Mass from Identified Electrons</b> | <b>26</b> |
| 7.1. Additional Cuts Used  | 26        |
| 7.2. Background Source: $Z^0 \rightarrow \tau\bar{\tau}$                 | 28        |
| 7.3. Background Source: $Z^0 \rightarrow q\bar{q}$ , jets from quark     | 30        |
| 7.4. $Z^0$ Resolution  | 31        |
| <b>8. Conclusion</b>   | <b>32</b> |
| <b>References</b>  | <b>34</b> |



## 1. INTRODUCTION

The Large Hadron Collider (LHC) located at Geneva, Switzerland, will be the biggest particle accelerator in the world. There are a number of detectors on the LHC ring. The LHCb [6] detector is aimed to study bottom quark physics, which will allow a measurement of the parameters of CP violation in bottom quark productions. The ALICE experiment [2] is specialized in Pb+Pb heavy ion collisions. The ATLAS [3] detector is a general purpose detector, and it will be conducting p+p collision experiments. In addition, the Compact Muon Solenoid (CMS) [4] is currently being commissioned. It will start taking data from as early as late 2008. The detector will be excel in muon detection, but it is also a general purpose detector for p+p and Pb+Pb collisions. The CMS experiment opens up a new window into physics at a unprecedented energy.

With the new energy range, a lot of exciting new physics can be examined. The search for the HIGGS boson, which arises from scalar field and is postulated to account for the mass of vector bosons, is one of the main goals of the experiment. The energy range of the LHC is well matched for either confirming its existence or ruling it out. The LHC experiments also want to research on super-symmetry, which potentially explains a lot of open questions for physics beyond the standard model.

Although the CMS detector will devote most of its time running proton-proton collisions, one month of each year it will be running lead-lead collisions at center-of-mass energy of 5.5 TeV. Through heavy ion collisions more about the properties of the quark-gluon plasma can be studied, like the viscosity or opacity. In preparation

for further studies to the lead-lead collisions, it is interesting to test the basic detector capabilities by studying basic particle reconstruction capabilities. Reconstruction of prompt photon in the heavy ion background has been studied by the MIT heavy ion group last summer [9], and it leads to the main goal of this thesis. Electrons are one of the main background of the photons, and certainly an important particle type that future studies might need.

Inside the CMS detector there will be a roughly constant magnetic field 4.0 Tesla maintained by a superconducting magnet, which allows good measurement of the particle momentum. A slice of the detector is shown in Figure 1. The detector consists of several parts, from inside to outside there are silicon trackers, electromagnetic calorimeter (ECAL), hadronic calorimeter (HCAL), and finally the muon chambers. The tracker is specialized of measuring the momentum of charged particles. The particles will leave a trace on the tracker as they fly through the detector. One important feature about the readout of the tracker is that the output is not binary. Instead, it has an multiple-bit ADC value which allows for better measurement of the direction and better identification of the particle that passes through the tracker. This makes the tracker good for heavy ion events. The electromagnetic and hadronic calorimeters measure energies of different types of particles. Particles such as electrons and photons will deposit most of its energy into the electromagnetic calorimeters, whereas hadrons dump most of their energy into the hadronic calorimeter. The measurement of missing energy in hadronic calorimeter also provides signature of new particles.

This study will be focused on the reconstruction of electrons in heavy ion back-

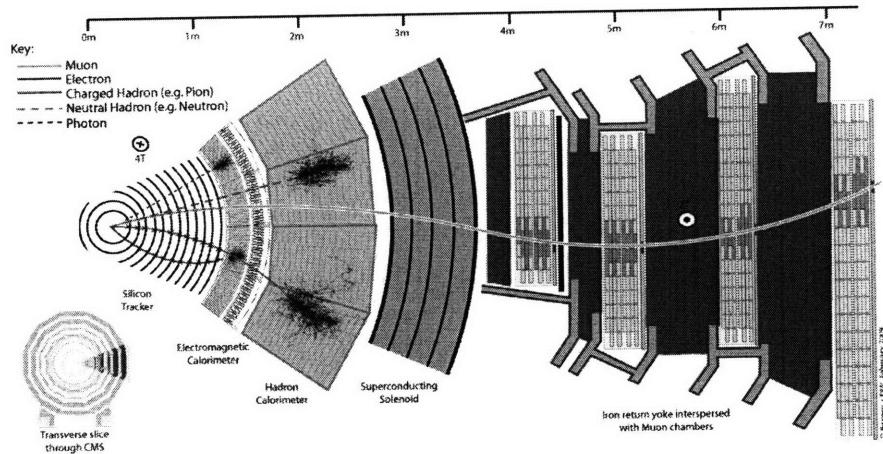


FIG. 1: A slice of the CMS detector [1]. From inside-out there are silicon trackers, electromagnetic calorimeter, hadronic calorimeter, superconducting magnet and muon chambers.

ground. The reconstructed electrons are then used to show that the reconstruction of the invariant mass of  $Z^0$  boson in heavy ion background is possible. The expected number for various particles is listed in section 2. In section 3 the simulated samples used for the study. In the following two sections the reconstruction procedure and the reconstruction properties for electrons. In section 6 the background sources to electrons and the reconstruction of  $Z^0$  are discussed. Last but not least, additional cuts used for  $Z^0$  reconstruction and the results are written in section 7.

## 2. PRODUCTION RATES AT LHC

Because of the higher energy, the production rates of high transverse momentum particles are much larger than in previous experiments. The production rate for  $Z^0$  bosons in p+p collision at 14 TeV is shown in Figure 2. The production rates of various particles at LHC for central Pb+Pb collision at  $\sqrt{s_{NN}} = 5.5 TeV$  are estimated and

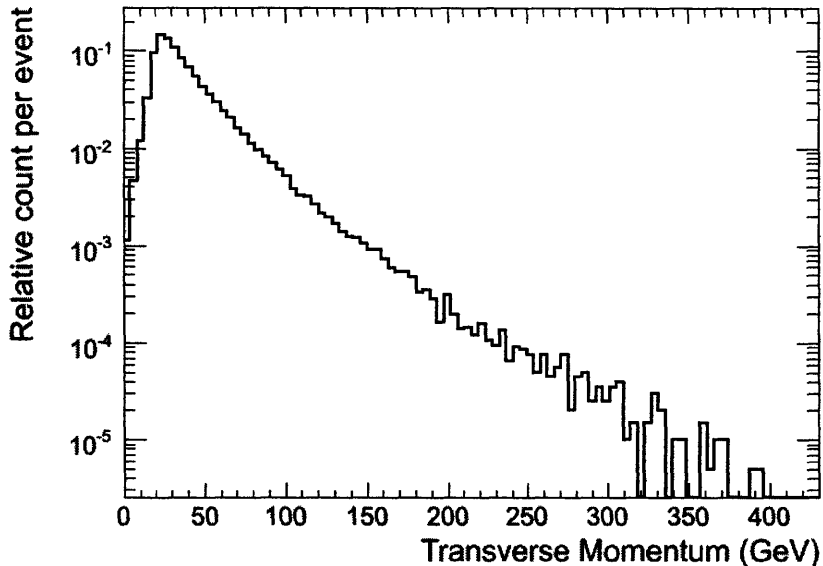


FIG. 2: Expected production rate of  $Z^0$  boson per event estimated from Pythia generator plotted as a function of transverse momentum.

shown in Figure 3 from the Hydjet generator [10].

### 3. SIMULATED SAMPLES

For the purpose of this study, we simulated a number of different types of events:

1. Pythia events [11] with  $Z^0$  to  $e^+e^-$  decay enforced. To study electron reconstruction and to check that the reconstruction is working, Pythia events containing  $Z^0$  are simulated, and the  $Z^0$  boson is forced to decay into an electron-positron pair. In this way, one can obtain the distribution of the electron energies as they will appear in the real experiment. The large mass of the  $Z^0$  boson also makes it a perfect target to check the electron reconstruction. The large mass will cause it to decay into high energy electrons, and high energy electrons are easier to

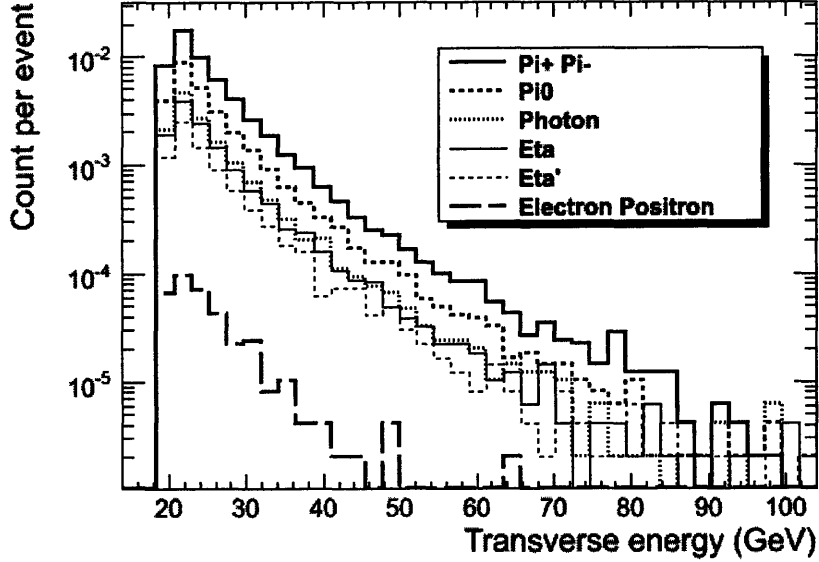


FIG. 3: Expected production rate of background particles from central Pb+Pb collision events at LHC from Hydjet generator plotted as a function of transverse momentum.

detect. The parameters used to generate these events are shown in table I.

The electron transverse energy distribution from the samples can be found in

Figure 4.

TABLE I: Parameters used to generate Pythia samples with  $Z^0 \rightarrow e^+e^-$ .

| Parameter       | Value | Comment  |
|-----------------|-------|--|
| MSTU(21)        | 1     | Check on possible errors during program execution                |
| CKIN(3)         | 20    | ptHard min   |
| CKIN(7)         | -3    | y min  |
| CKIN(8)         | 3     | y max  |
| MSEL            | 0     | User defined processes   |
| MSUB(15)        | 1     | $q\bar{q} \rightarrow gZ^0$                                      |
| MSUB(30)        | 1     | $qg \rightarrow qZ^0$  |
| MSTP(43)        | 2     | $Z^0$ only   |
| MDME(174 ~ 179) | 0     | $Z^0$ decaying into quark-antiquark pair                         |
| MDME(182)       | 1     | $Z^0$ decaying into electron-positron pair                       |
| MDME(183 ~ 187) | 0     | $Z^0$ decaying into lepton pair other than electron and positron |

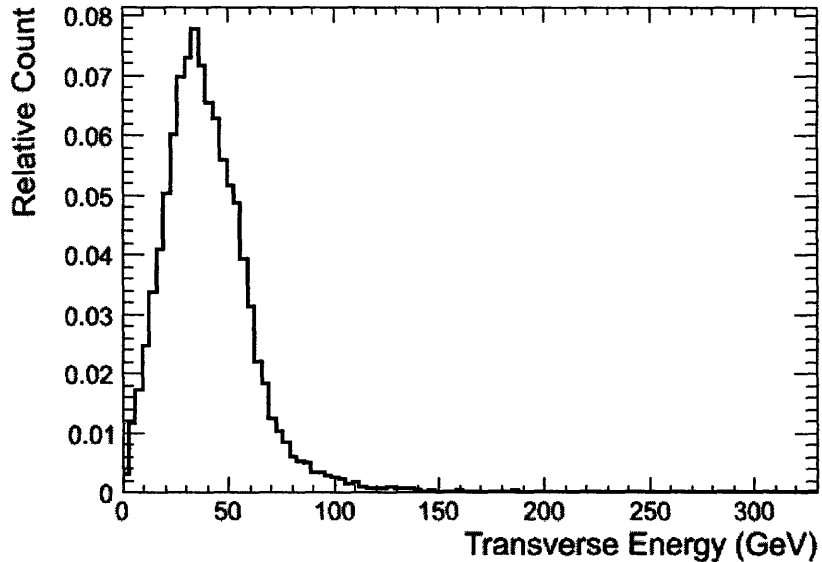


FIG. 4: The transverse energy distribution of the electrons coming from  $Z^0$  boson from the Pythia generator.

## 2. Particle gun

The particle gun is a simple event generator that generates an event with a certain number of particles of specific types at certain region of momentum space. This is useful in studying the detector response to a certain particle type.

## 3. Central Hydjet events

The Hydjet generator [10] is used to generate background events to simulate the heavy ion background. It simulates Pb+Pb events of  $\sqrt{s_{NN}} = 5.5 TeV$ . In this study, we use central events with impact parameter  $b = 0$ . In the analysis, we mix these events with the signal events we want to study (either Pythia events or particle gun events). The process of mixing will be discussed in the next subsection. The parameters used in production is listed in table II.

TABLE II: The parameters used to generate Hydjet events [9].

| Parameter | Value             | Comment   |
|-----------|-------------------|---|
| Mult      | $2.6 \times 10^3$ |   |
| Ytfl      | 1                 | max transverse flow rapidity  |
| Ylfl      | 3.75              | max longitudinal flow rapidity  |
| Part      | 1                 | fraction of event multiplicity proportional to number of participants |

### 3.1. Simulation, Mixing and Digitization

First we generate the events from, for example, the Pythia generator [11]. Then GEANT4 [8] is used to simulate the interaction of the particles with the detector material. The digitization step is needed to simulate the detector response to the simulated particles. In the case of studying events with heavy ion background, we mix the simulated particles of the target events which we want to study, for example p+p events containing  $Z^0$  to electron-positron pair, with the generated and simulated heavy ion events, and then redo the digitization since the detector response might not be linear in terms of the deposited energy.

The main reason that we are doing this is because of the large computation time for simulation. It took on average 65.3 seconds to simulate a Pythia event, and it will take too much time to generate and simulate lead-lead events differently for every thing we want to study, as the time needed for simulating a central Pb+Pb event is even even higher. It took about 20000 seconds per event.

## 4. RECONSTRUCTION PROCEDURE

After mixing and digitization is done, we move on to reconstruct various higher level objects. From the ECAL crystals we reconstruct energy clusters which measure the electron energies, and from the silicon tracker we reconstruct charged tracks. It turned out that the tracking algorithm is not yet ready for reconstructing electron tracks in heavy ion events, but there are other application for the tracks which will be introduced in a moment. After reconstruction, we then apply several cuts to rule out the candidates that are not created by electrons. Then, since there will be overall background in the lead-lead collision events, background subtraction is applied. Finally, in the case of studying the mass resolution of  $Z^0$  boson from the electron pair channel, back-extrapolation from the ECAL is performed to get the initial momentum of the electrons.

### 4.1. Supercluster Reconstruction

The main algorithm for electromagnetic calorimeter clustering used in this study is the island clustering algorithm in CMS software framework [7]. This algorithm first finds high enough energy crystals which are called the seeds, and then from the highest seed the algorithm searches around the seed crystal for crystals that are lower in energy and includes them in the cluster. It stops upon encountering a crystal that is higher in energy compared to its neighbor crystal within the cluster. The cluster produced this way is called the “basic cluster”. Then the whole algorithm is run again on the basic clusters to generate the “superclusters.”

There is also the hybrid clustering algorithm presenting in the standard CMSSW modules. However the algorithm doesn't perform as well in heavy ion events. The main reason is that there is an overall background in these events, and when the hybrid algorithm tries to decompose the energy in one crystal to different clusters, it gets confused.

#### 4.2. Tracker Reconstruction for Electrons

The biggest challenge of tracker reconstruction for electrons is Bremsstrahlung. Electrons are very light and are likely to emit photon on the way as they pass through the detectors. The emitted photons, as it turned out, are not too much of an issue in calculating the energy since the superclusters are relatively large and collect the energy efficiently as will be shown in the next subsection. The tracker, however, is different since the radiation from an electron will cause it to lose energy and subsequently change its direction and confuse the reconstruction algorithm, especially in heavy ion events, where a large amount of background particles are present.

Another issue of the standard p+p tracking algorithm is that it won't run fast enough for lead-lead collisions. Of course it is run offline, but it is still too slow. For a typical central ( $b = 0$ ) lead-lead event, the run time can easily go up to several hours, which renders the algorithm infeasible. A tracking algorithm specifically for heavy ion events is developed by Vasundhara Chetluru et al. Although the overall time efficiency is now much better (in order of minutes), the reconstruction efficiency for electron is still low. Again, please refer to the next subsection for plots.

So, tracker reconstruction is not used for measuring electron momentum in this study, although the reconstructed hadron tracks are used in electron isolation. The algorithm performs fairly well with other particle types.

### 4.3. Cuts Used to Select Electrons

There will be no generator information in the real experiment, and therefore we cannot know which clusters are generated by electrons. Therefore it is important to come up with some criteria to help reject the clusters from other particles while keeping the electron clusters. From the properties of the electron, the following cuts are used:

1. HCAL energy to ECAL energy ratio

Ideally, electrons will deposit all their energy into the electromagnetic calorimeter, while depositing no energy into the hadronic calorimeter. Therefore the energy ratio between these two types of calorimeters could serve as a good indicator to rule out super clusters created from a variety of different particle types. Hadrons will have a high hadronic calorimeter readout, and therefore by demanding the ratio to be close to zero we can rule out the hadrons. A plot showing the ratio of HCAL/ECAL for electron clusters and hadronic clusters is shown in Figure 5.

2. Cluster shape information

The cluster shape information is also important in determining the particle type that creates the cluster. Among the shape-related parameters,  $e3x3/e5x5$  is es-

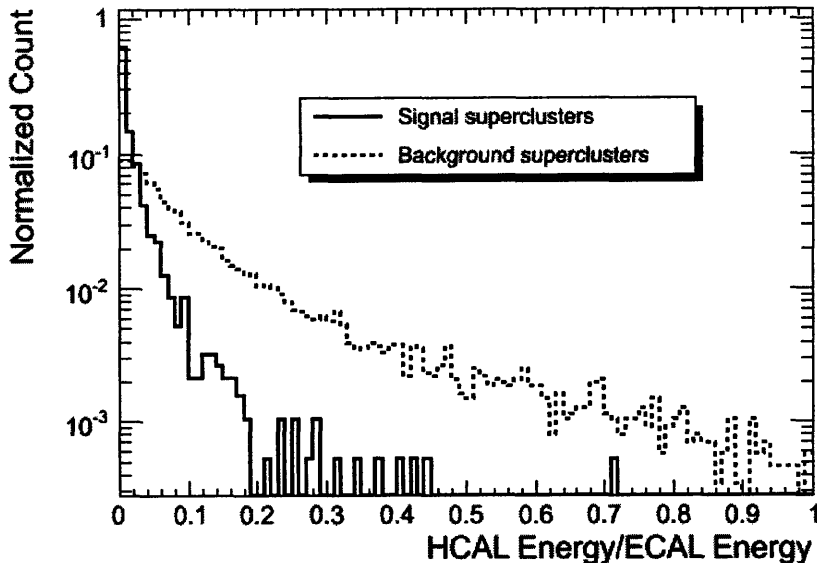


FIG. 5: HCAL energy to ECAL energy ratio between signal electron clusters and clusters from background particles in a central Hydjet event. The signal clusters are from electrons from a  $Z^0 \rightarrow e^-e^+$  decay.

pecially useful in finding electron clusters.  $e_{3 \times 3}$  is defined as the sum of energy of the 9 crystals closest to the center point of the cluster.  $e_{5 \times 5}$  is also defined similarly: the energy sum of the closest 25 crystals. A typical electron cluster is shown in Figure 6. As can be seen from the graph, the electron energy, despite the emission of bremsstrahlung, is still pretty concentrated. The location for the electron is also not too much off from the “perfect” location if there was no Bremsstrahlung effect, as shown in Figure 7. The  $e_{3 \times 3}/e_{5 \times 5}$  distribution for electron clusters is shown in Figure 8.

### 3. Isolation

In collision events, jet can be produced by many processes such as high energy quarks. The scattered quarks fragment into a cascade of different particles, and

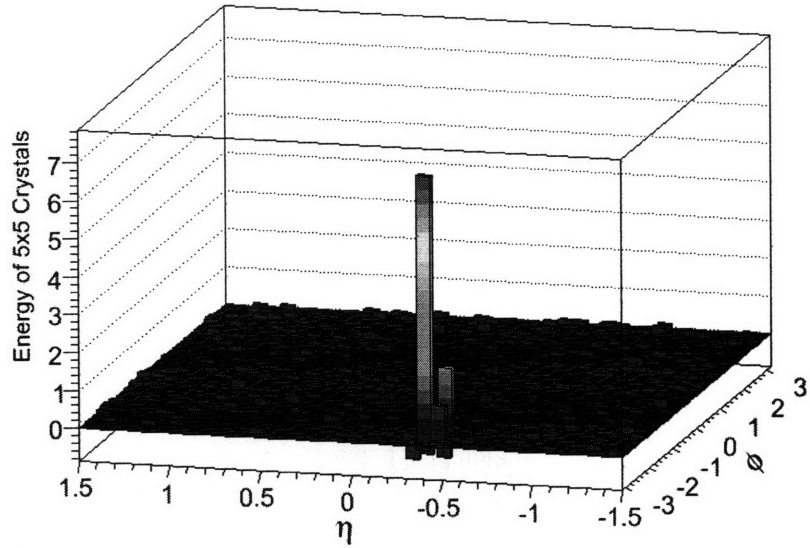


FIG. 6: A typical cluster shape of electron. Each bin in the figure is a unit of 5x5 ECAL crystals, and this is generated from a single-electron event.

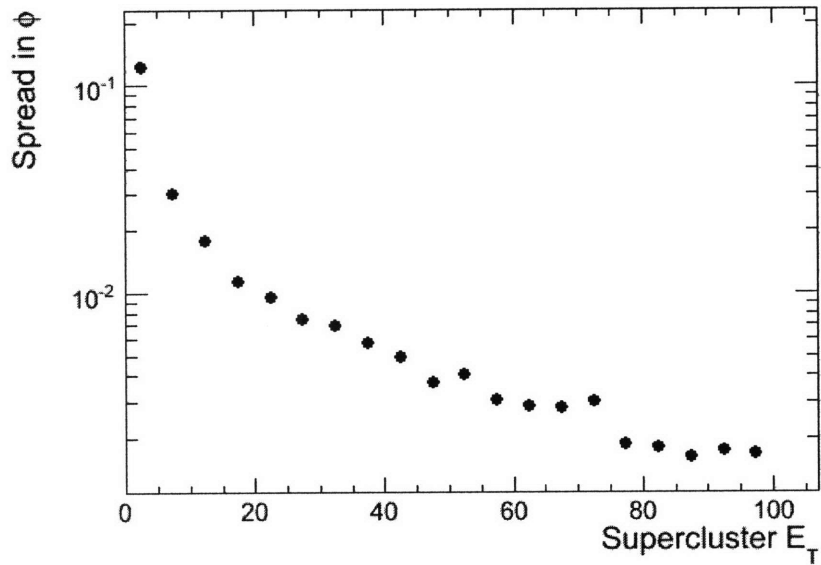


FIG. 7: The spread (RMS) in  $\phi$  of hitting point on the ECAL surface from electrons due to the Bremsstrahlung effect.

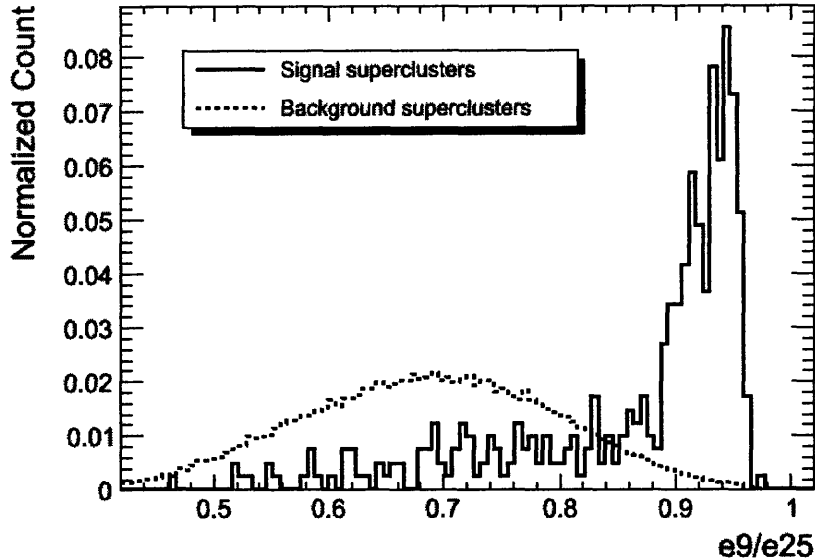


FIG. 8: A comparison of energy concentration, calculated as the ratio of the energy of the closest 9 crystals to the energy of the closest 25 crystals, across clusters between background clusters and clusters from signal electrons.

there is some possibility that some components of the jet will be misidentified as an electron and contribute to background. Therefore it is useful to see what is around the ECAL cluster. If there are a lot of tracks in the same  $\eta$ ,  $\phi$  region, it is more likely to be part of the jet, and less likely to be one of the electrons we want to find. A number of parameters are introduced, defined similarly to the parameters in the gamma-jet studies [9].  $Txy$  is defined as the number of tracks with transverse momentum greater than  $3y$  GeV within a cone with size  $0.1x$ . The size is calculated in  $\eta - \phi$  space.  $dRxy$  is defined as the  $y$ -th closest track with transverse momentum greater than  $0.4x$  to the cluster. This gives us a series of parameters, and the comparison between electron clusters and background clusters for some of the parameters are shown in Figure 9.

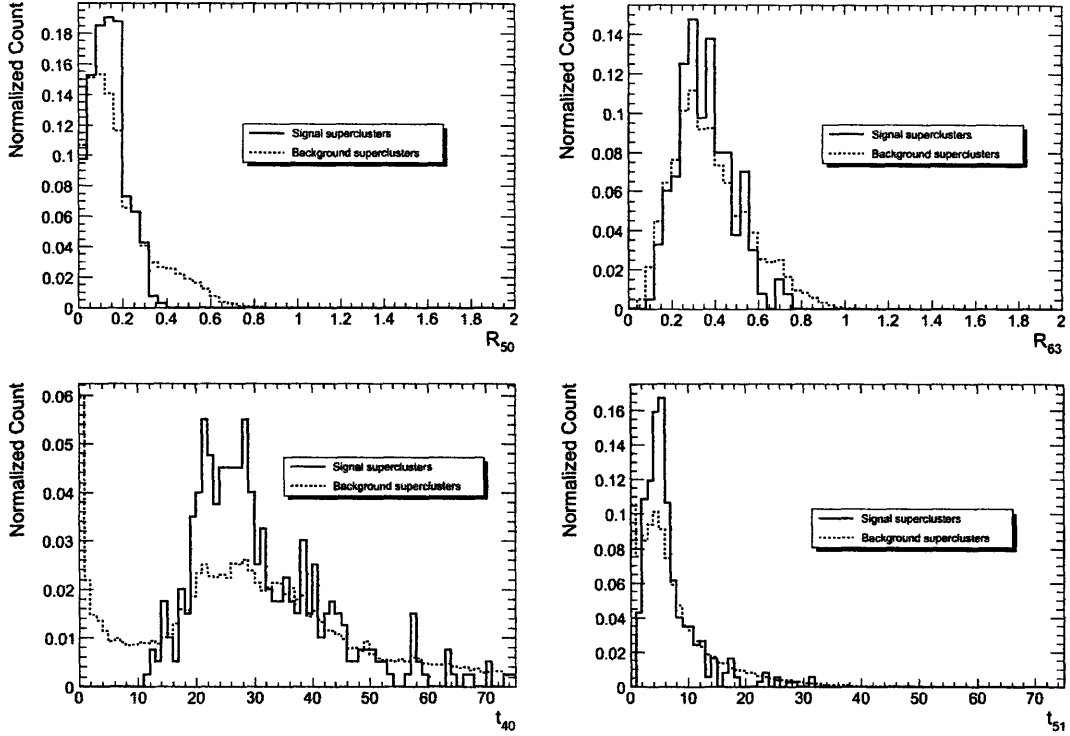


FIG. 9: The isolation parameters. Only 4 of the parameters are shown here. The solid lines are the electron clusters, and the dotted lines are the background. The curves are normalized. Not all of the parameters are useful, but some of them certainly show good isolation power.

#### 4. Making Final Cut

The final cut is determined by finding the maximum of the significance for each of the cuts. The significance is defined as the number of signal clusters surviving the cut divided by the square root of all clusters after the cut. Each cut is decided separately, and then all the cuts are applied together to reject the background clusters.

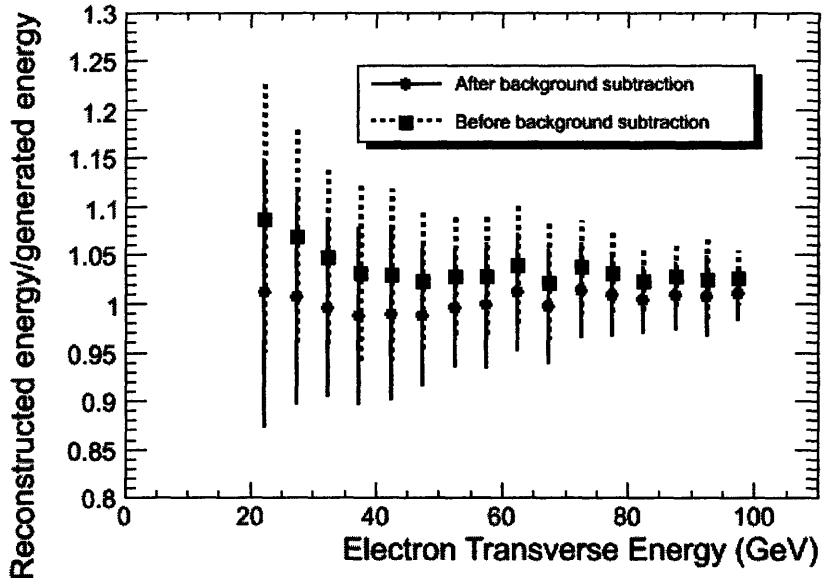


FIG. 10: The ratio between reconstructed energy and generated energy, before and after background subtraction assuming flat background. The error bar consist of the statistical error and systematic error which comes from the resolution of the ECAL crystals.

#### 4.4. Background Subtraction

Since there are a lot of background particles in central heavy ion collision events, an energy correction on top of the existing energy correction in the clustering algorithm is needed to get a better measurement of the electrons. As shown in Figure 10, assuming flat background energy in each crystal performs well in central heavy ion events. The term flat refers to a uniform energy distribution of background events in  $\eta - \phi$  space.

#### 4.5. Back-extrapolation

Since there is no tracking information and the only information we have is the magnitude of the momentum, the starting vertex of the electron has to be assumed.

Even if we are reconstructing electron pair together, the information is still not sufficient for finding the correct vertex.

However, for high transverse energy electrons, the amount of angle change from the center of the detector to the ECAL surface is relatively small. The angle change relative to transverse momentum is shown in Figure 11. One ECAL crystal has size  $0.0156 \times 0.0156$  in barrel region, so a charged particle with transverse momentum greater than about 50 GeV will be hit at the same ECAL crystal as if the particle had no charge. From this we can estimate the error caused by assuming a primary vertex for the electrons.

For moderate to high transverse energy electrons, the error in measured transverse energy caused by the shift of the producing vertex is estimated to be at most 0.6 percent at  $\eta = \pm 1$  if the vertex is shifted 2 cm along the colliding axis from the center of the detector.

## 5. SIMPLE RECONSTRUCTION PROPERTIES

### 5.1. Electromagnetic Calorimeter

The following plots are done by particle gun events. In order to understand the reconstruction better, several aspects of the electron reconstruction is discussed.

Particles with various different energy is shoot towards the ECAL crystals, and then we compare the reconstructed clusters versus the generator information. The efficiency and reconstructed energy to original energy comparisons are plotted in Figures 12 and

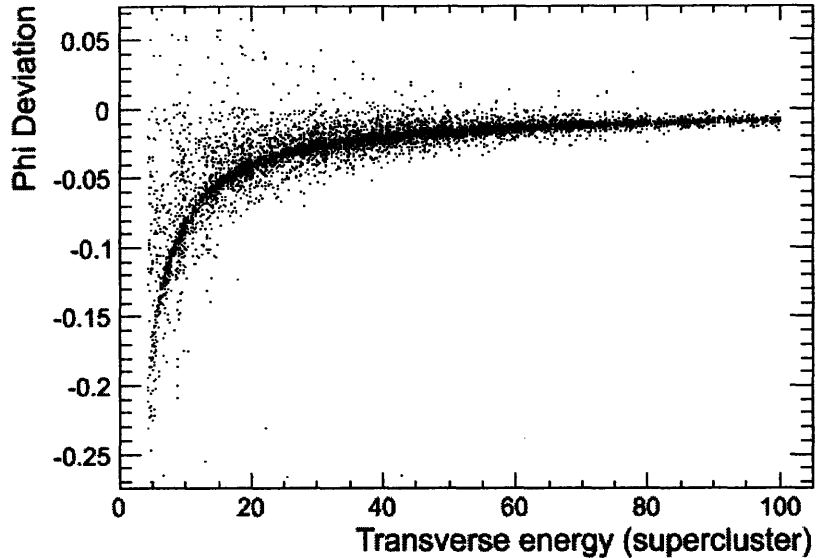


FIG. 11: The deviation in  $\phi$  of an electron between starting direction (at center of detector) and the ending direction on the ECAL surface.

13. The energy resolution is pretty good for all electrons with transverse energy greater than 20 GeV, and the efficiency is greater than 90 percent with  $E_T > 30$ .

## 5.2. Electron

As a check of the degree of Bremsstrahlung, the percentage of electrons which are collected in a single cluster is plotted versus transverse energy of the electron. It is shown in Figure 14. Comparing this plot with the energy resolution plot (Figure 13), we can see that most of the electrons don't lose too much energy due to radiation and that the radiated energy won't interfere with the energy measurement of the electrons from the electromagnetic calorimeter.

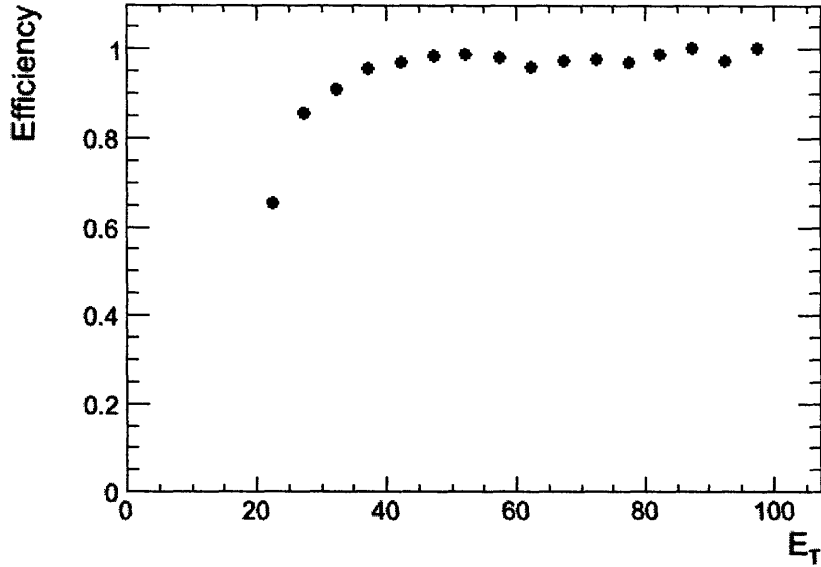


FIG. 12: The efficiency of the clusters from electrons in central Pb+Pb background.

### 5.3. Electron tracking in Heavy ion Background

It is also worth mentioning the reconstruction properties of tracking for electrons in the heavy ion background. The Figures 15 and 16 show the efficiency and performance for electron tracking. The algorithm used is specialized in heavy ion tracking overall, but not specifically tuned for electrons. Therefore the efficiency for electron track reconstruction is pretty low, especially because of the large amount of background tracks around. In p+p collisions, the tracker reconstruction algorithm works better. Although the radiation changes the direction of the electron a bit, the algorithm has higher success rate of finding back the right points.

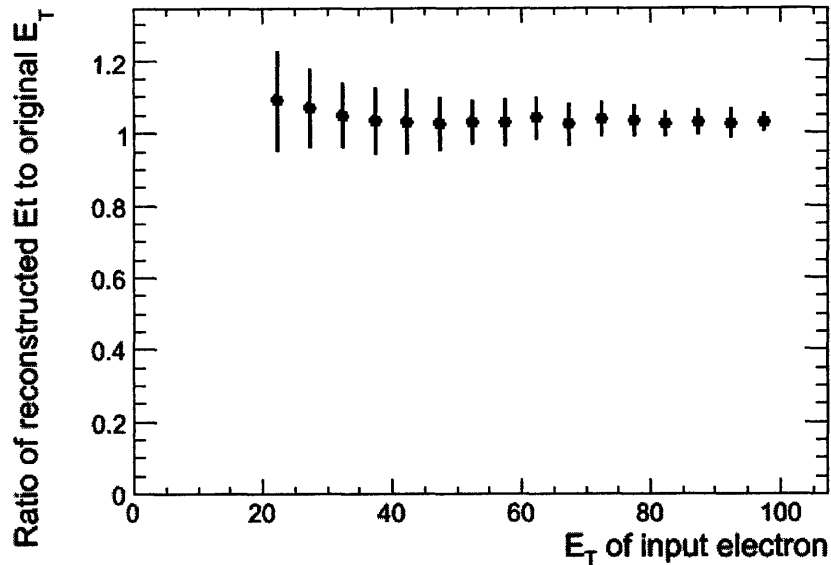


FIG. 13: The cluster energy resolution of the clusters from electrons in central Pb+Pb background. The reconstructed energy is higher because of the heavy ion background.

## 6. BACKGROUND PARTICLES

One of the most common background particles that might be misidentified as electrons are photons. Both electron and photon have similar properties on the electromagnetic calorimeter. One can check whether there is a charged track pointing towards the supercluster; however, until the tracking algorithm for electrons is improved or a new algorithm is implemented, the two particle types are usually not separable. On the other hand, most other particle types can be filtered out from one of the cuts.

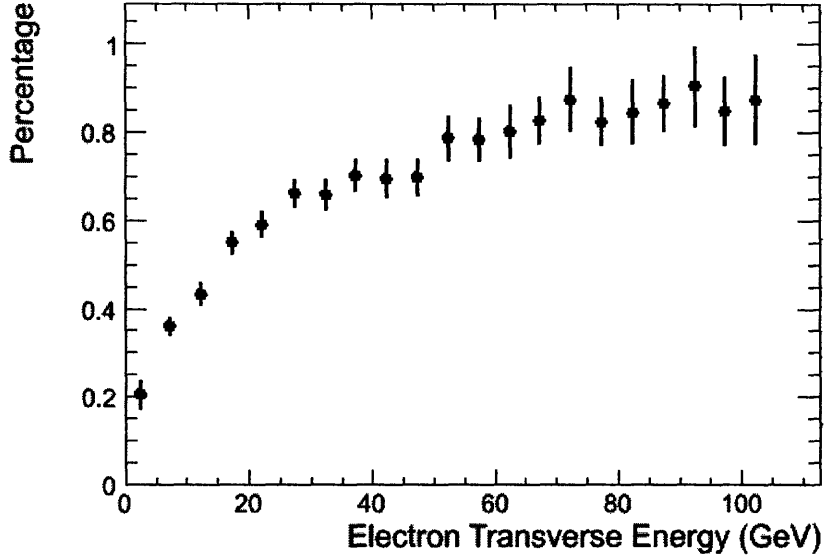


FIG. 14: The rate of electrons of which more than 90 percent of its energy being captured by a single cluster as a function of transverse energy.

## 7. RECONSTRUCTING $Z^0$ MASS FROM IDENTIFIED ELECTRONS

### 7.1. Additional Cuts Used

#### 1. Transverse energy

The electrons from  $Z^0$  boson have high energy. In addition, the mother particle of the electrons,  $Z^0$ , has nonzero transverse momentum, so there will be less low transverse momentum electrons. On the other hand, the noise clusters will mostly have low transverse energy, which makes it a good candidate for a cut. The comparison plot between electron clusters from  $Z^0$  boson versus random clusters is shown in Figure 17. One can also cut on transverse momentum on the combined electron pair, which from the distribution of  $Z^0$  boson transverse momentum we know that there aren't many  $Z^0$ 's with low transverse energy.

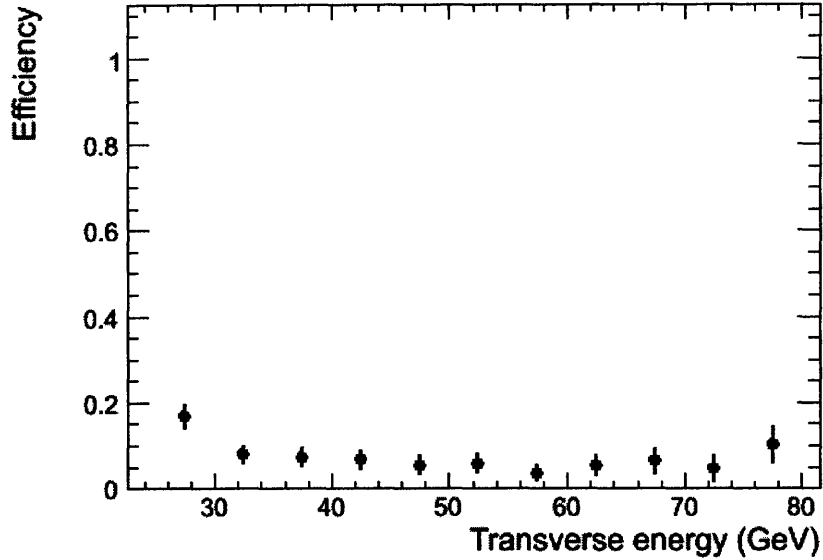


FIG. 15: Electron track efficiency as a function of electron transverse energy in central Pb+Pb background.

## 2. Energy correlation between two electrons

Since the leptons come from the same mother particle, there will be correlations in energy of the electron and positron (see Figure 18 for the transverse energy scattering plot of the electrons). Pretty much the same reason as before, since the  $Z^0$  boson has nonzero transverse energy, there is less probability that the resulting lepton will have low energy. Therefore if we calculate the ratio of energy difference to energy sum, we can expect that the ratio is higher at low values and less so closer to one. On the contrary, there are a lot of low transverse energy background clusters, and there will be more background pairs with the energy ratio close to one. A comparison plot between signal leptons and background clusters is shown in Figure 19

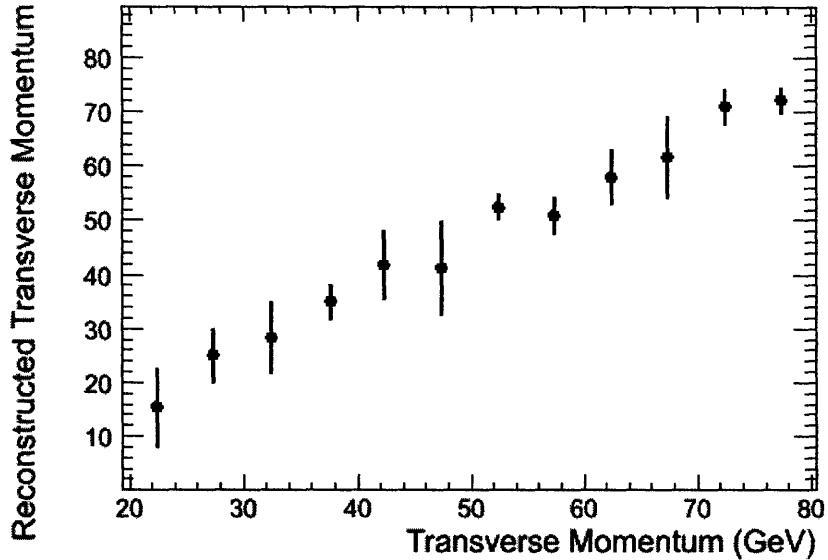


FIG. 16: Electron track momentum resolution as a function of transverse momentum of the electron. The resolution is measured with a central Pb+Pb background.

### 3. $\phi$ correlation between electrons

The angle difference between the leptons is also an important indicator of whether the supercluster pair is from  $Z^0$  boson or not. It turned out that due to the mass of  $Z^0$ , the  $\phi$  angle between the daughter leptons are in most cases large, whereas the background cluster pairs don't have an correlation in angles and are therefore flat in distribution. The comparison plot is shown in Figure 20.

### 7.2. Background Source: $Z^0 \rightarrow \tau\bar{\tau}$

During the one-month heavy ion run in CMS,  $Z^0$  bosons will produce abundantly. It is estimated that the number of  $Z^0$  will be around  $10^5$  at mid-luminosity [5]. Among them, about 3 percent will decay into  $\tau$ , and subsequently decay

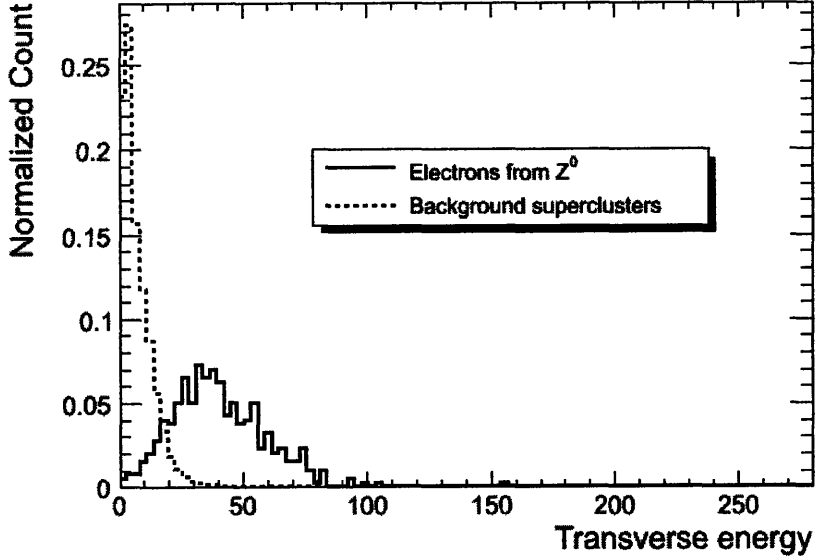


FIG. 17: The transverse energy of the electron clusters and the background clusters from central heavy ion events.

into various different particles, including particles that might leave a trace on electromagnetic calorimeter. For the purpose of reconstructing  $Z^0$  mass, this will be the largest electroweak background source. However, since there are always byproduct coming out together with the electrons from  $\tau$ , the energies of the electrons are smaller than the ones from  $Z^0 \rightarrow e^-e^+$  channel directly. Therefore, the angle between the misidentified electrons and the energy difference to energy sum ratio will be different, and consequently be filtered out.

The  $Z^0$  boson mass, reconstructed in the same way as in the electron pair channel, is shown in Figure 21. The “peak”-like structure appearing at about 40 GeV is an artifact of the  $E_T > 20$  GeV cut for the electron and positron. One thing to note is that the number of electron pairs passing through the cuts is very small compared to the efficiency in  $Z^0 \rightarrow e^-e^+$  events. Therefore, although the slope

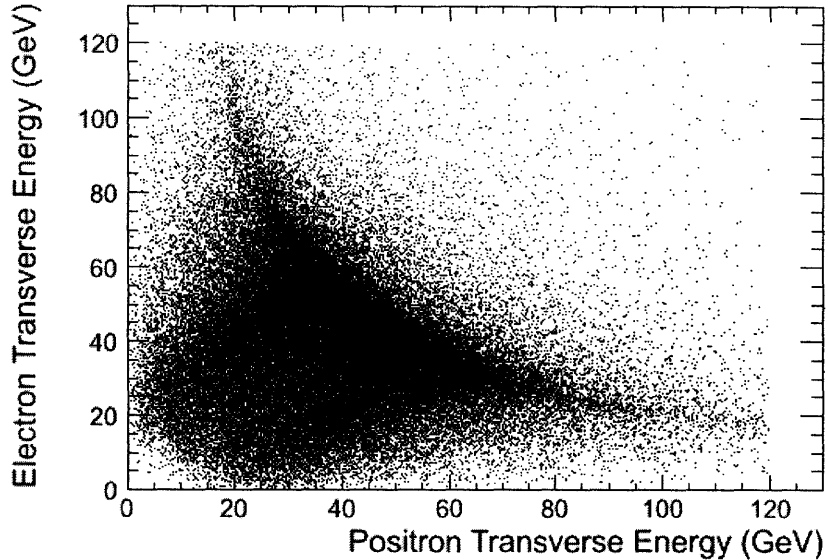


FIG. 18: Correlation between positron and electron transverse energy originating from the same  $Z^0$  boson.

of the reconstructed curve might introduce a bias to the mass of  $Z^0$  boson we measured from the electrons, it is safe to ignore and assume a small uncertainty if the number of available events is not large enough to see the baseline.

### 7.3. Background Source: $Z^0 \rightarrow q\bar{q}$ , jets from quark

Another big source of background particles come from the jets which decays from various heavy particles. As with the case of  $Z^0 \rightarrow \tau\bar{\tau}$ , one of the fragments in the jet might as well be a low energy electron and interfere with the target we would like to study.

However, since there will be a lot of jet fragments around the misidentified particle, the isolation cuts will prefer the isolated electron over the ones in jets. As

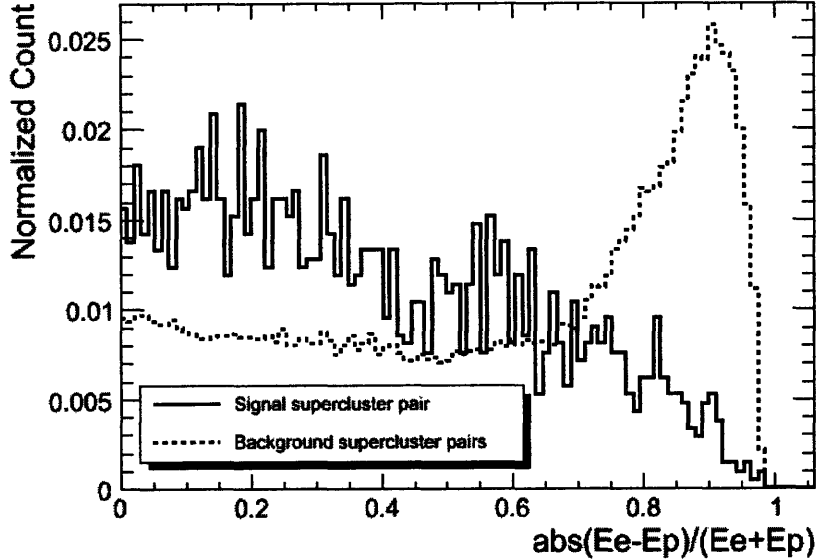


FIG. 19: Energy difference over the summation of energy of the positron-electron pair coming from  $Z^0$ . The dotted line shows the distribution of the background cluster pairs.

a result some of the signal electrons might be lost, but we can cut out most of the misidentified particles from jets.

#### 7.4. $Z^0$ Resolution

The mass distribution of the electron pairs, after reconstruction and cuts as described in the previous subsections, is shown in Figure 22. After baseline subtraction, the width (half width at half maximum) of the peak is 6.79 GeV, whereas the width from the generator level is 2.08 GeV.

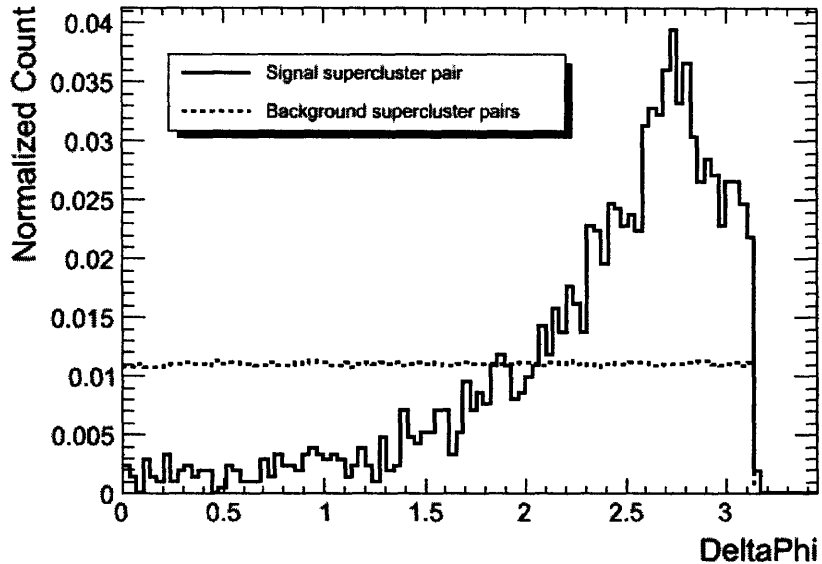


FIG. 20: Delta phi correlation between electron-positron pair from  $Z^0$ .

## 8. CONCLUSION

Several aspects of electron reconstruction in the lead-lead collision environment have been studied. Although the tracking algorithm is not yet ready for reconstructing electrons, we demonstrated that the calorimeters alone are capable of picking out high transverse energy electrons using the selection criteria that were developed in this thesis. Using these selected electrons, it is also shown that from the calorimeters alone one can reconstruct the invariant mass of the  $Z^0$  boson. This will be an important new observable in heavy ion collisions at the LHC, complementing studies of  $Z^0$  production in the di-muon channel. For future improvement, one could design a modified algorithm to search for electron tracks, allowing better discrimination between electron clusters and photon clusters.

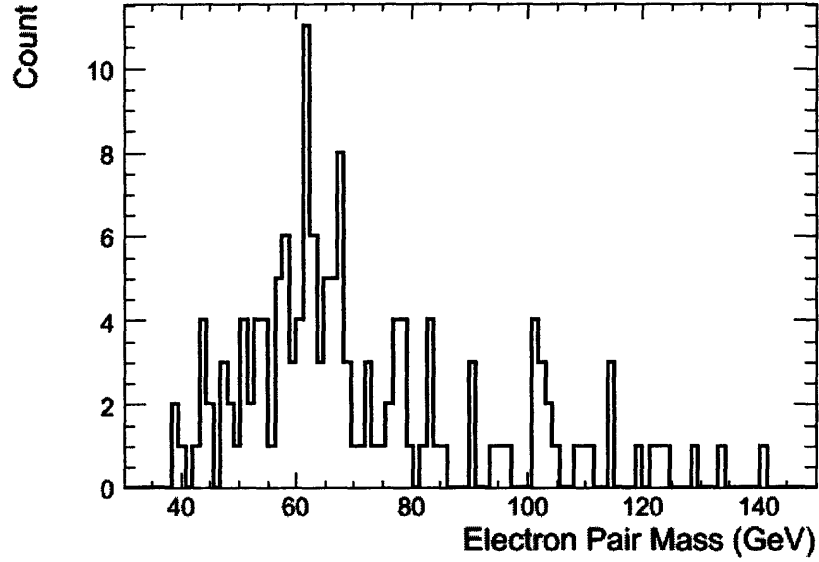


FIG. 21: Reconstructed electron pair mass from misidentified electrons in  $Z^0 \rightarrow \tau\bar{\tau}$  events. This plot is generated from 750000 events.

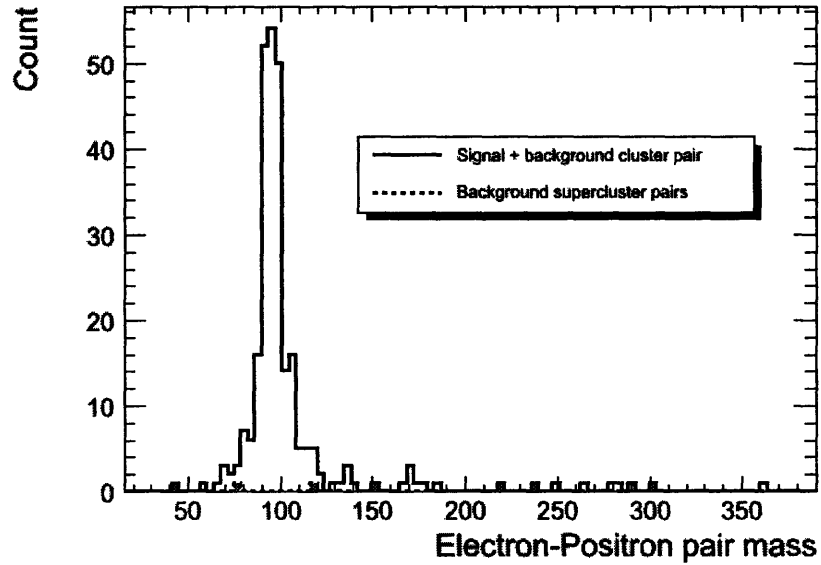


FIG. 22:  $Z^0$  resolution plot from the signal events of  $10^6$ s run of Pb+Pb events at  $\sqrt{s_{NN}} = 5.5$  TeV.

- 
- [1] A transverse slice of the cms detector. source: Cms outreach.
- [2] The ALICE Collaboration. Technical proposal. *CERN/LHCC*, 95-71, 1995.
- [3] The ATLAS Collaboration. Atlas detector and physics performance. *CERN/LHCC*, 99-14, 1999.
- [4] The CMS Collaboration. The compact muon solenoid - technical proposal. *CERN/LHCC*, 94-38:290, December 1994.
- [5] The CMS Collaboration. Cms physics technical design report: Addendum on high density qcd with heavy ions. *J. Phys. G: Nucl. Part. Phys.* 34 2307-2455, 2007.
- [6] The LHCb Collaboration. Lhcb technical proposal. *CERN/LHCb*, 98-4, February 1998.
- [7] E. Menschi et al. Electron reconstruction in the cms electromagnetic calorimeter. *CMS Note*, 2001/032:16, June 2001.
- [8] S. Agostinelli et al. Geant4 - a simulation toolkit. *Nuclear Instruments and Methods A* 506 250-303, 2003.
- [9] Y. Chen et al. Study of photon-tagged jet events in high-energy heavy ion collisions with cms. *CMS Analysis Note AN-2007/051*, 2008.
- [10] A.M. Snigirev I.P. Lokhtin. Fast simulation of flow effects in central and semi-central heavy ion collisions at lhs. *arXiv:hep-ph/0312204v2*, 2004.
- [11] P. Skands T. Sjostrand, S. Mrenna. Pythia 6.4 physics and manual. *JHEP* 0605 026, 2006.